General Disclaimer

One or more of the Following Statements may affect this Document

- This document has been reproduced from the best copy furnished by the organizational source. It is being released in the interest of making available as much information as possible.

- This document may contain data, which exceeds the sheet parameters. It was furnished in this condition by the organizational source and is the best copy available.

- This document may contain tone-on-tone or color graphs, charts and/or pictures, which have been reproduced in black and white.

- This document is paginated as submitted by the original source.

- Portions of this document are not fully legible due to the historical nature of some of the material. However, it is the best reproduction available from the original submission.

Produced by the NASA Center for Aerospace Information (CASI)

N O T I C E

THIS DOCUMENT HAS BEEN REPRODUCED FROM MICROFICHE. ALTHOUGH IT IS RECOGNIZED THAT CERTAIN PORTIONS ARE ILLEGIBLE, IT IS BEING RELEASED IN THE INTEREST OF MAKING AVAILABLE AS MUCH INFORMATION AS POSSIBLE

METALLURGICAL AND MATERIALS ENGINEERING

University of Pittsburgh
Pittsburgh, Pennsylvania 15261

HOT CORROSION OF Co-Cr, Co-Cr-Al,

AND Ni-Cr ALLOYS IN THE

TEMPERATURE RANGE OF 700 - 750°C

Third Semi-Annual Report
on
Grant No. NSG-3214

Prepared for

National Aeronautics and Space Administration

Lewis Research Center

by

K. T. Chiang

G. H. Meier

Department of Metallurgical and Materials Engineering
University of Pittsburgh
Pittsburgh, Pennsylvania 15261

TABLE OF CONTENTS

1.0 Introduction

Coatings based on the Co-Cr-Al system are now widely used in marine aircraft turbines. They are known to have excellent hot corrosion resistance at normal turbine operation temperatures (900-100?°C). However, they are subject to severe degradation at lower temperatures (700-800°C) which can occur when the turbines are operating at low power or at particular locations on turbine components which normally fall into this temperature range.

Considerable uncertainty still exists regarding the mechanisms of this form of corrosion despite several careful investigations. The corrosion morphology corresponding to low temperature hot corrosion has been well characterized on components removed from marine services[1,2]. The attack is primarily of a pitting type with the oxide in the pits enriched in Cr and Al in alternating layers and depleted in Co. A Co-rich oxide covers the pits. There is little or no sulfidation in the alloy and generally no depletion of β-CoAl below the oxide pit. A thin zone at the base of the pit is found to contain S, Al, and O in a phase (or phases) which are apparently not water soluble. Small amounts of water soluble Co have also been observed on corroded coatings and the oxide pits are permeated by Na_2SO_4 which is also water soluble. Barkalow and Pettit were able to reproduce this morphology at 700°C by exposing CoCrAlY coatings with Na_2SO_4 deposits to oxygen containing SO_3 at pressures greater than 10^{-4} atm. The rate of degradation was found to be proportional to the SO_3 pressure and negligible in the absence of SO_3. These observations have been incorporated into the following mechanism by Pettit and co-workers[1,3]. The reaction of CoO and SO_3 forms $CoSO_4$ which forms a low melting point solution with Na_2SO_4. The liquid salt then penetrates the

Al_2O_3 scale at cracks. Alternating layers of Al and Cr are formed by selective removal of Al from the alloy presumably by Al-sulfite formation at the liquid/alloy interface where the p_{O_2} is low and then reprecipitation as oxide where the p_{O_2} is higher. The Al-depleted alloy is converted to Cr_2O_3 to form the Cr-rich region and Co which diffuses to the liquid/gas interface forming Co-oxide or sulfate. It is suggested[1,3] that this mode of attack is not operative at high temperatures because much higher SO_3 pressures are required to form sulfates and sulfites.

Smeggil[2], on the other hand, suggests that the corrosion morphology may be reproduced in the absence of SO_3 in the gas phase if the coatings are exposed to brief thermal excursion and transient reducing conditions and proposes this an an alternate mechanism. Laboratory hot corrosion experiments in which specimens were periodically cycled to 1300°C for 30 seconds in carbonaceous material produced corrosion morphologies similar to those observed in marine turbines and have produced changes in coating microstructure similar to those observed by Smeggil in marine turbine components. Smeggil does not offer a mechanism for the degradation produced by the high temperature excursions.

Luthra and Shores[4] have studied the low temperature hot corrosion of Co-30Cr and Co-10Al alloys between 600 and 750°C. They find that Co-30Cr undergoes a pitting type of attack in the presence of SO_3. The pit contains Cr_2O_3 and Na_2SO_4 with a sulfur-rich band at the alloy/scale interface and an external scale of Co_3O_4 or $CoSO_4$, depending on the SO_3 pressure. The Co-10Al alloy showed uniform attack rather than pitting but its corrosion morphology was otherwise analogous to that for Co-30Cr. The mechanism proposed by Luthra and Shores includes the formation of a liquid Na_2SO_4-$CoSO_4$ phase as a

result of reaction between transient CoO and SO_3. The rapid dissolution of Co into this salt is proposed to prevent the formation of a continuous Cr_2O_3 or Al_2O_3 film.

Studies at the University of Pittsburgh[5] have shown that the introduction of SO_3 into gas phase results in pitting-type hot corrosion of both Co-27Cr and Co-18Cr-6Al alloys giving corrosion morphologies similar to those described above. Higher SO_3 pressures were required to form pits on the Co-Cr alloy and thermal cycling resulted in pitting of both alloys at lower SO_3 pressures. The presence of NaCl in the gas also produces a pitting type of attack in Na_2SO_4-coated Co-Cr-Al which is somewhat similar to that produced by SO_3. However, a major difference was a porous microstructure produced below the pit by the formation of volatile chlorides of Al and Cr which were transported outward through the pores and converted to oxide in regions of higher p_{O_2}.

The objective of the research described in this report was to more clearly define the effects of SO_3, alloy composition, and alloy microstructure in the early stages of the Na_2SO_4-induced hot corrosion of Co- and Ni-based alloys in the temperature range 700-750°C.

2.0 Experimental

The alloys studied were Co-27Cr, Ni-20Cr, and Co-18Cr-6Al*. The alloys were tungsten arc melted under an argon atmosphere. Specimen coupons were cut from the alloys, polished through 600 grit silicon carbide and cleaned ultrasonically. Sodium sulfate coatings were applied by spraying with aqueous solutions while the coupons were heated using a hot plate and a heat lamp. Coating weights were usually 1 mg/cm^2

---

*All concentrations expressed in weight percent.

although some thinner coatings were also used.

The specimens were exposed in tube furnaces to oxygen at 1 atm. The SO_3 pressure in the gas was controlled by using O_2-SO_2 mixtures or by passing O_2 through a permeation tube apparatus to introduce small amounts of SO_2 and passing the gas over a Pt catalyst to establish the SO_2/SO_3 equilibrium.

The specimens' weight changes were determined by weighing them before and after exposure. The oxidized specimens were studied using optical and scanning electron metallography, EDAX, and X-ray diffraction . The salt was washed from selected specimens and analyzed by atomic absorption spectroscopy at NASA Lewis Research Center.

3.0 Experimental Results and Discussion

3.1 Co - Cr and Ni - Cr Alloys

Figure 1 shows a cross-section through a pit typical of those observed on binary Co-Cr alloys. This specimen was exposed with a 1 mg/cm^2 coating of Na_2SO_4 for 48 hours at 750°C in oxygen in which the P_{SO_3} was 5.8×10^{-3} atm. Table 1 indicates the presence of SO_3 caused a 40-fold larger weight change for the alloy compared with O_2. The micrograph and X-ray maps indicate a thick external scale of cobalt oxide covering a pit containing Cr_2O_3 with a sulfur-rich region at the pit base. Some penetration of fingerlike corrosion product is also evident below the scale/alloy interface. Figure 2 shows more detail of these protrusions below a similar pit. The sulfur map, Figure 2d, indicates a significant concentration of sulfur in the protrusions. Point count EDAX analysis indicates the matrix between the protrusions is partially depleted of Cr. It, therefore, appears this region is depleted of Cr by the formation of Cr_2O_3 in the pit and the formation of the protrusions which are sulfides (and, perhaps, oxides) of Cr. (It must be pointed

out that the identification of the protrusions is tentative.)

The above results suggest a sulfidation/oxidation mechanism to be a major contributor to the pit formation in Co-Cr alloys. The corrosion process is envisiged as follows. The high SO_3 pressure in the gas phase results in the formation of a liquid Na_2SO_4-$CoSO_4$ solution which locally dissolves the protective external Cr_2O_3 scale. (The higher SO_3 pressure required to induce this mode of attack in Cr_2O_3-forming as compared with Al_2O_3-forming alloys is indicative of the lower solubility of Cr_2O_3 in acid melts[6].) The molten salt penetrates below the scale. The conditions of low P_{O_2} and high P_{S_2} established at this location result in the dissolution of Co which is transported outward until it precipitates as Co oxide where the P_{O_2} is higher and the formation of Cr sulfides. The combination of disruption produced by the rapid dissolution of Co and localization of Cr in sulfides prevents a continuous Cr_2O_3 scale from reforming.

Figure 3 shows severe corrosion at the corner of a Ni-20Cr specimen exposed under the same conditions as the Co-Cr alloy in Figures 1 and 2. The specimen has gained about ten times more weight than that exposed in the absence of SO_3, Table 1. In this case considerable quantities of Cr sulfide are present at the scale-alloy interface. Figure 4 shows a micrograph and X-ray images of the corrosion product on the same specimen. Nickel may transport through a liquid Na_2SO_4-$NiSO_4$ melt (There is an eutectic between the extended solid solution of $NiSO_4$ in Na_2SO_4 and $NiSO_4 \cdot Na_2SO_4$ at about 670°C, 35% $Mo/NiSO_4$.) and precipitate as NiO or $NiSO_4$ near the gas interface. Chromium remains essentially below the initial alloy/salt interface and is oxidized in-situ. The EDAX spectrum of Figure 3d verifies that the outer regions of the pit are rich in Cr, Ni, and S. The result coupled with the micrograph,

Figure 3c, suggest this region consists of Cr_2O_3 and Ni-sulfide, e.g.
point A on the stability diagrams for the Cr-S-O and Ni-S-O systems,
Figures 5 and 6. These results suggest the sulfidation and subsequent
oxidation of Cr prevents a Cr_2O_3 scale from forming in the attacked
region of this alloy also.

3.2 Co - Cr - Al Alloys

Figure 7 shows the morphology of a pit formed in Co-18Cr-6Al
exposed to O_2 with $P_{SO_3} = 2 \times 10^{-3}$ atm. for 48 hours at 750°C with a
Na_2SO_4 coating. The pit is rich in Al and Cr with a Co-rich external
layer and S-enrichment at the pit base. Water-soluble Co was found on
the surfac of similar alloys, particularly after longer times under
thermal cycling conditions. An additional feature of this figure is
preferential attack of the β-CoAl phase. Figure 8 shows this feature
for an earlier stage of the pit formation . The β is preferentially
attacked and appears to provide a path for more rapid propogation of
the corrosion product into the alloy than is available through the solid
solution phase. It should be pointed out that the round shape of the
pit in this figure may be the result of a sectioning effect through a
pit propogating in three dimensions. The more rapid attack along the
Al-rich, Cr-free phase may be consistent with the greater solubility of
Al_2O_3 in acid melts as compared with Cr_2O_3[6].

The observations of the corrosion morphologies for the Co-Cr-Al
alloys do not lead to a clear mechanism. The sulfite mechanism pro-
posed by Pettit and co-workers[1,3] can explain the observed behavior.
However, thermochemical calculations for Na-sulfite indicate this com-
pound never appears as a stable compound at unit activity in the tempera-
ture range under consideration[7]. Data are not available for Al-sulfite
and this compound has not been found in the literature. However, the

possibility of forming Al-sulfite at less than unit activity in Na_2SO_4 is a possibility and could allow the observed corrosion behavior to be explained. More work is needed in clarifying this mechanism.

The sulfidation/oxidation mechanism proposed in the previous section for Co-Cr and Ni-Cr could also explain the behavior. However, sulfides have not been observed at the pit base in the present investigation. This mechanism may be responsible for the pitting behavior observed by Smeggil[2] when specimens were exposed under transient reducing conditions in the absence of SO_3. These conditions will cause the sulfur potential in the salt to become very high and may well initiate pitting corrosion via the sulfidation/oxidation mechanism observed for binary Co-Cr alloys.

Finally, it must be remarked that similar pitting morphologies may be generated by a number of mechanisms. As noted earlier[5], the presence of NaCl vapor can produce pitting of Na_2SO_4-coated Co-Cr-Al although additional features in the form of porosity arise in this case. A sulfidation/oxidation mechanism is observed to operate in binary Co-Cr alloys and pits may be produced in Co-Cr-Al both by high SO_3 pressures and by transient reducing conditions. Also, as seen in Figure 9 a Co-Cr-Al alloy may undergo pitting-type corrosion in the absence of a salt deposit[8] This specimen is a Co-18Cr-6Al-1Hf alloy exposed at 1000°C for 94 hours to a simulated coal gas in which $p_{O_2} \approx 10^{-15}$ atm. and $p_{S_2} \approx 2 \times 10^{-6}$ atm. ($p_{SO_3} \approx 10^{-15}$ atm.). The major factor determining whether or not pits form is the ability of the environment to continually prevent the formation of a protective scale at localized sites. However, the detailed features of the pits will generally be different for the different mechanism (e.g. the thick Co-oxide outer scale did not occur in Figure 9) and must be carefully evaluated before a mechanism can be prepared with confidence.

SUMMARY

The effect of SO_3 pressure in the gas phase on the Na_2SO_4-induced hot corrosion of Co-Cr, Ni-Cr, and Co-Cr-Al alloys has been studied in the temperature range 700 - 750°C. The degradation of the Co-Cr and Ni-Cr alloys was found to be associated with the formation of liquid mixed sulfates ($CoSO_4$-Na_2SO_4 or $NiSO_4$-Na_2SO_4) which provided a selective dissolution of the Co or Ni and a subsequent sulfidation/oxidation mode of attack which prevented the maintenance of a protective Cr_2O_3 film. A clear mechanism was not developed for the degradation of Co-Cr-Al alloys. The sulfite model proposed by Pettit and coworkers or a modification of the above sulfidation/oxidation mechanism are both capable of explaining the experimental results. Additional work is needed in this area. Finally it was illustrated that a pitting - corrosion morphology can be induced by a number of different mechanisms.

REFERENCES

1. R. H. Barkalow and F. S. Pettit, "On the Mechanism for Hot Corrosion of CoCrAlY Coatings in Marine Gas Turbines", paper presented at the 4th Conference on Gas Trubines in Marine Environments, Annapolis, MD, June, 1979.

2. J. G. Smeggil, "Study of the Effects of Gaseous Environments on the Hot Corrosion of Superalloy Materials", Quarterly Report to NASA Lewis Research Center on Contract NAS3-21376, December, 1978.

3. C. S. Giggins and F. S. Pettit, "Hot Corrosion Degradation of Metals and Alloys -- A Unified Theory", Pratt and Whitney Aircraft, Final Report to Air Force Office of Scientific Research on Contract No. F44620-76-C-0123, June, 1979.

4. K. L. Luthra and D. A. Shores, "Morphology of Na_2SO_4-Induced Hot Corrosion at 600-750°C", paper presented at 4th Conference on Gas Turbines in Marine Environments, Annapolis, MD, June, 1979.

5. G. H. Meier and E. A. Gulbransen, "Hot Corrosivity of Coal Gasification Products on Gas Turbine Alloys", Summary Report for the Period 15 April 1978 to 15 November 1979 on DOE Contract No. DE AC01-79-ET-13547, Jan. 1980.

6. W. P. Stroud and R. A. Rapp, "The Solubilities of Cr_2O_3 and α-Al_2O_3 in Fused Na_2SO_4 at 1200K", in High Temperature Metal Halide Chemistry, D. L. Hildenbrand and D. D. Cubricciotti, eds., Electrochem. Soc., p. 574 (1978).

7. K. T. Chiang, E. A. Gulbransen, F. S. Pettit, and G. H. Meier, unpublished research.

8. C. M. Packer, Lockheed Palo Alto Research Laboratory, unpublished research.

ACKNOWLEDGEMENT

TABLE 1: Weight Changes (mg/cm^2) After 48 Hrs, at 750°C

Gas Composition	O_2		O_2 + 1000 ppm SO_2 $P_{SO_3} = 6\times10^{-4}$ atm		O_2 + 1% SO_2 $P_{SO_3} = 6\times10^{-3}$ atm	
Alloy	No Salt	$1\ mg/cm^2$ Na_2SO_4	No Salt	$1\ \frac{mg}{cm^2}$ Na_2SO_4	No Salt	$1\ mg/cm^2$ Na_2SO_4
Co-20Cr	1.5	0.4	0.43	0.04	0.95	5.2
Co-27Cr	0.09	0.05	0	-0.13	0.09	1.9
Co-18Cr-6Al	0.05	-0.05	0.05	-.14	0.04	-17.6(S)
Co-18Cr-6Al-1Hf	0.1	0	0.13	0.44	0.06	-20.9(S)
Ni-20Cr	0.14	0.14	0.24	0.04	0.09	2.3

(S): Scale spalled off during cooling to room temperature

FIGURES
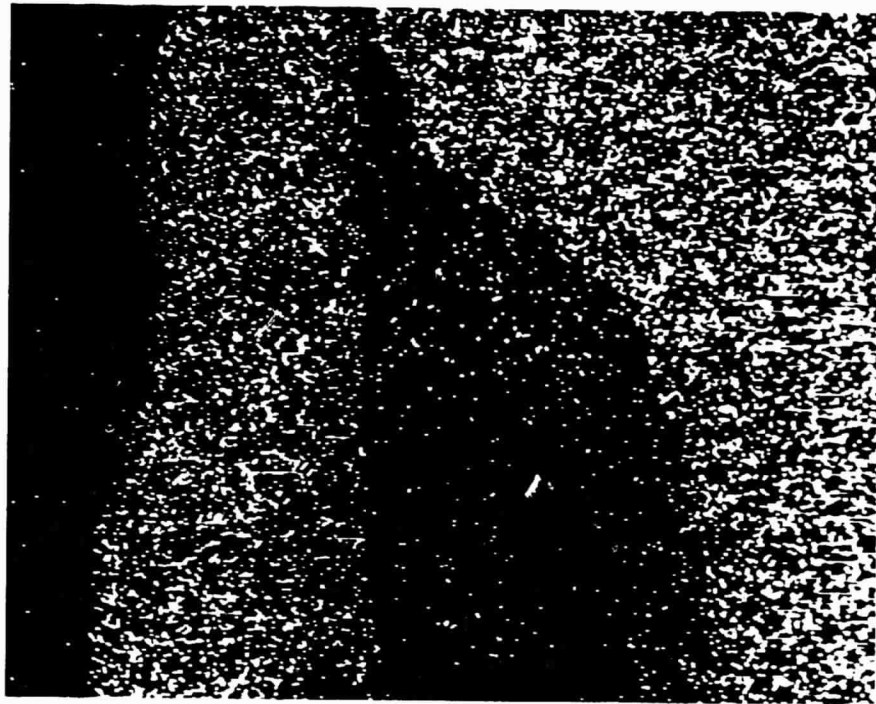
Figure 1. Corrosion morphology for Na_2SO_4-coated Co-27Cr exposed to O_2 + SO_3 (p_{SO_3} = 5.8 x 10^{-3} atm) for 48 hrs. at 750°C.

a. SEM micrograph. b. Co X-ray map. c. Cr X-ray map. d. S X-ray map.

d.

c.
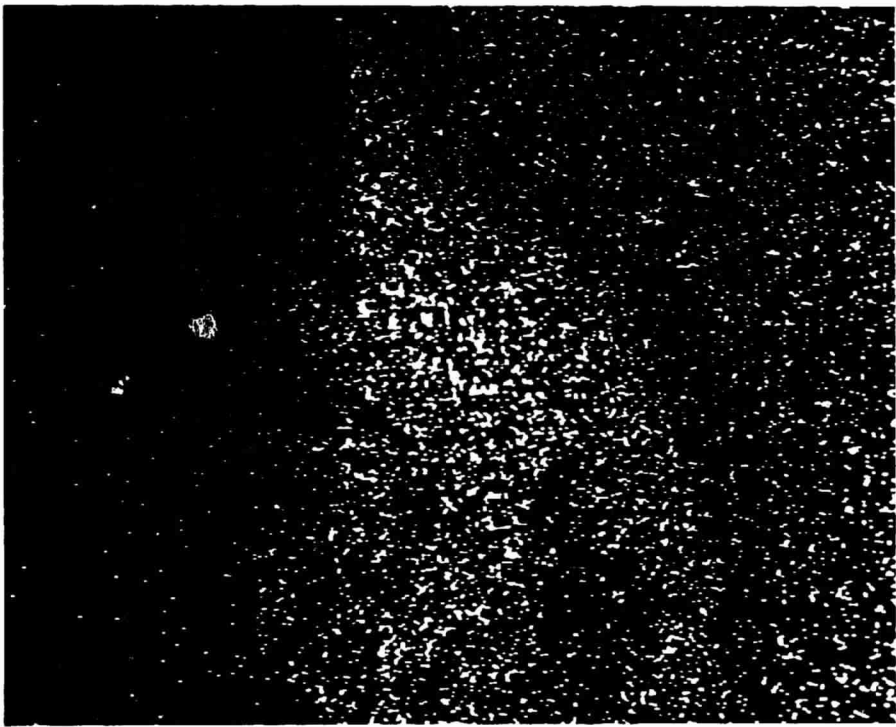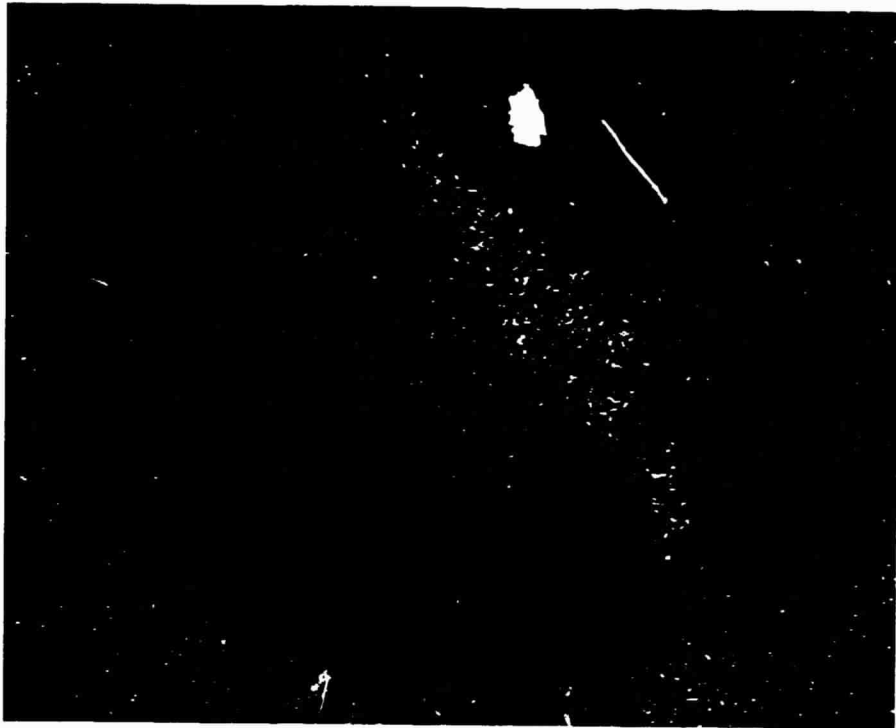
Figure 1. (Cont'd.)
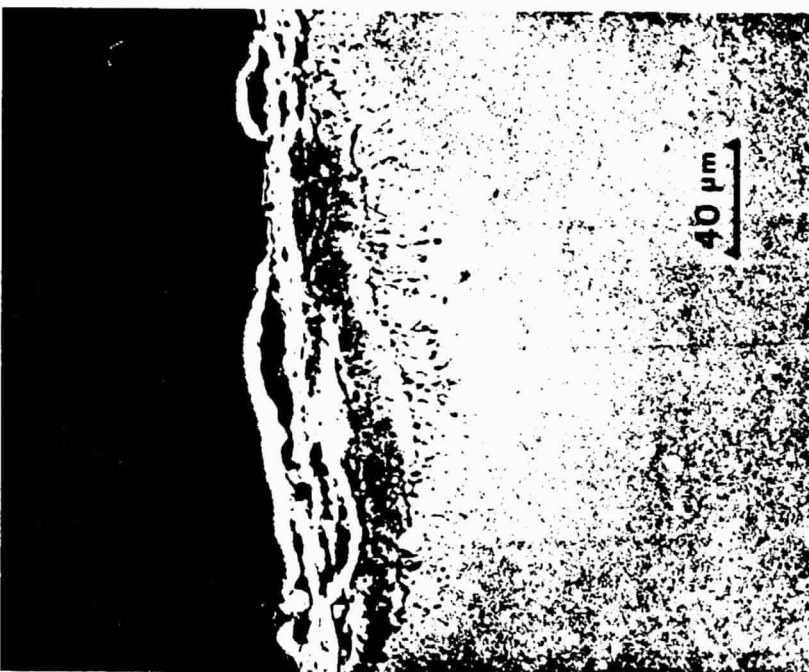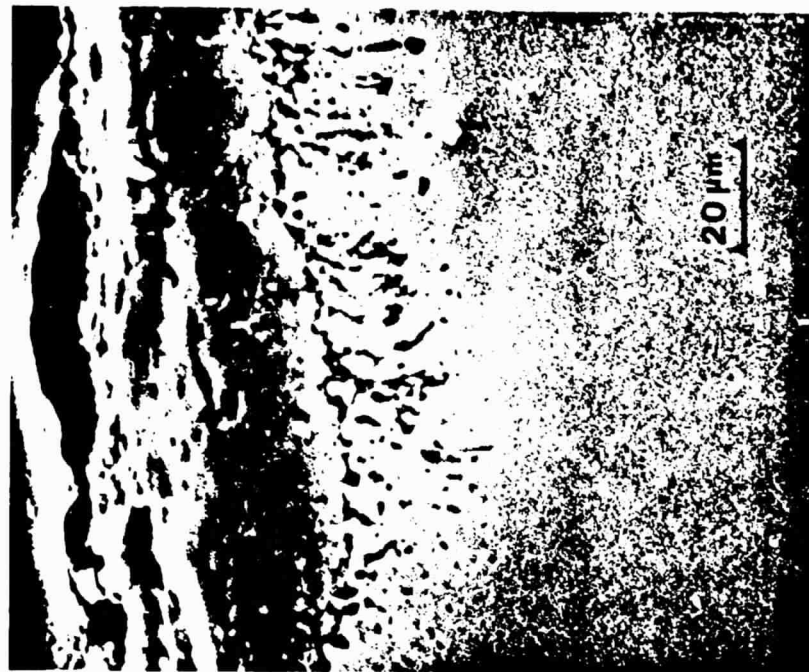
Figure 2. Scanning Electron Micrographs of the specimen in Fig. 1 showing more detail of the corrosion front morphology; a, b, c, and S distribution d.

d.

c

Figure 2. (Cont'd.)

a

b
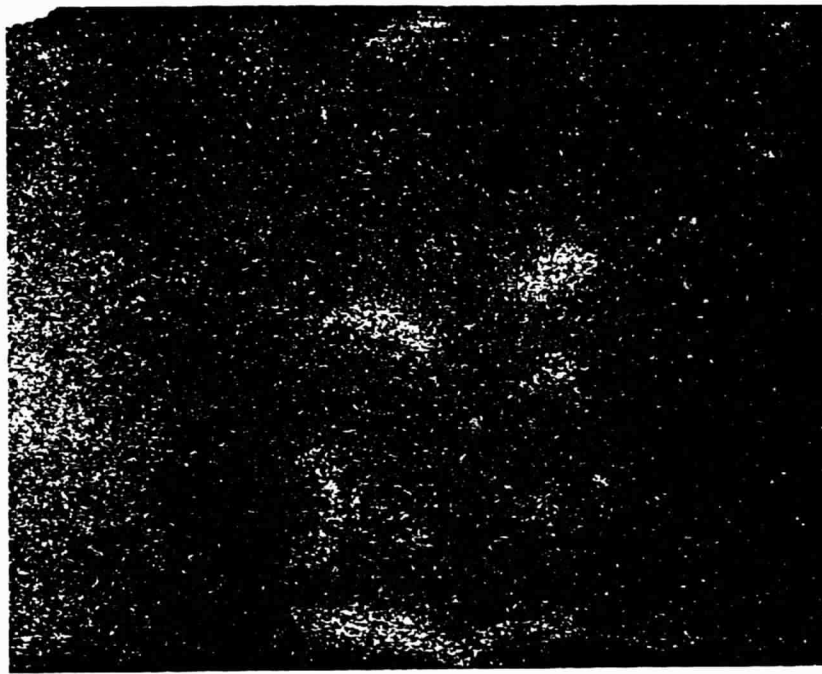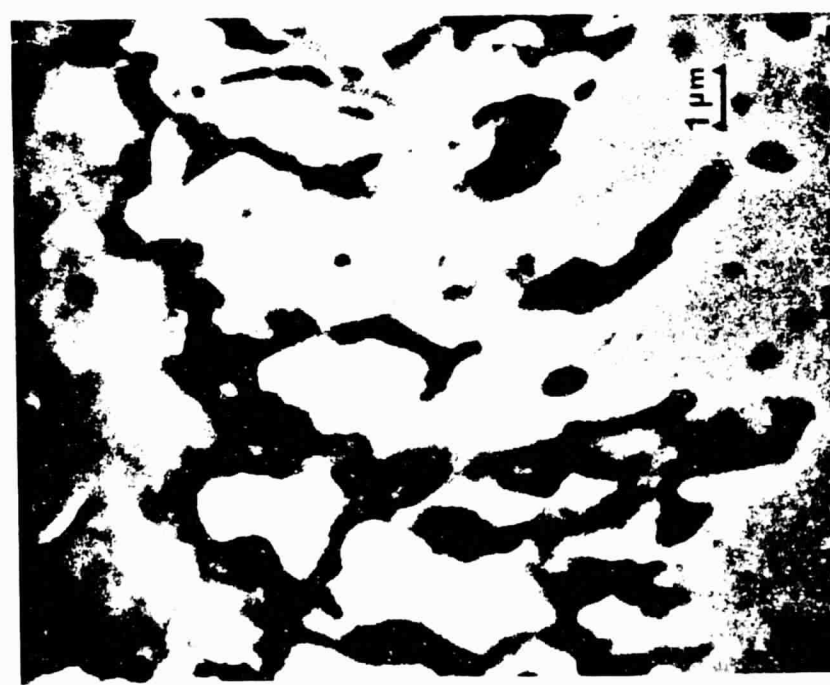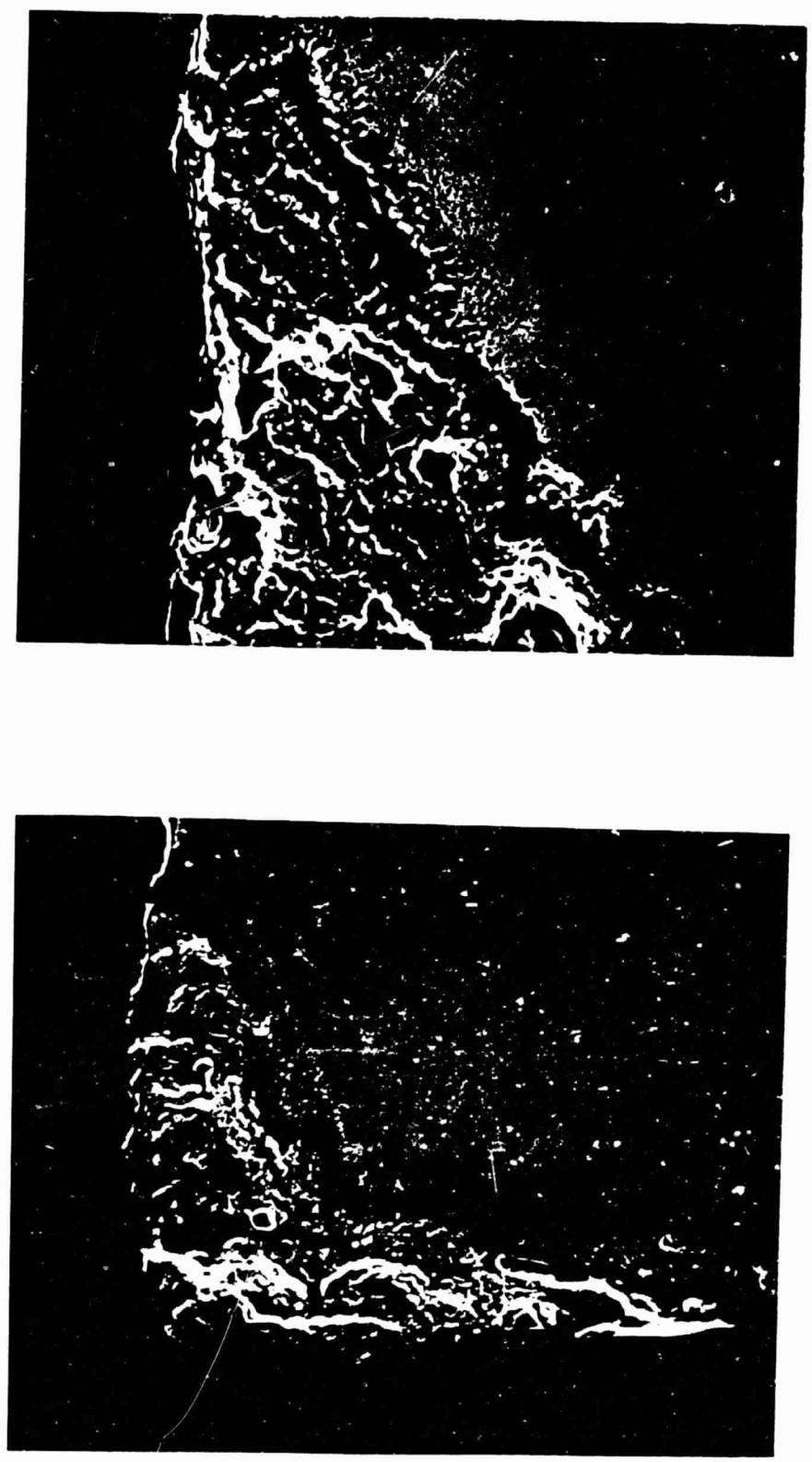
Figure 3. Corrosion morphology for Na_2SO_4-coated Ni-20Cr exposed to O_2 + SO_3 (pSO_3 = 5.8 x 10^{-3} atm) for 48 hours at 750°C.

a, b, c. SEM micrographs. d, e, f. EDAX spectra from the locations indicated in c.

c
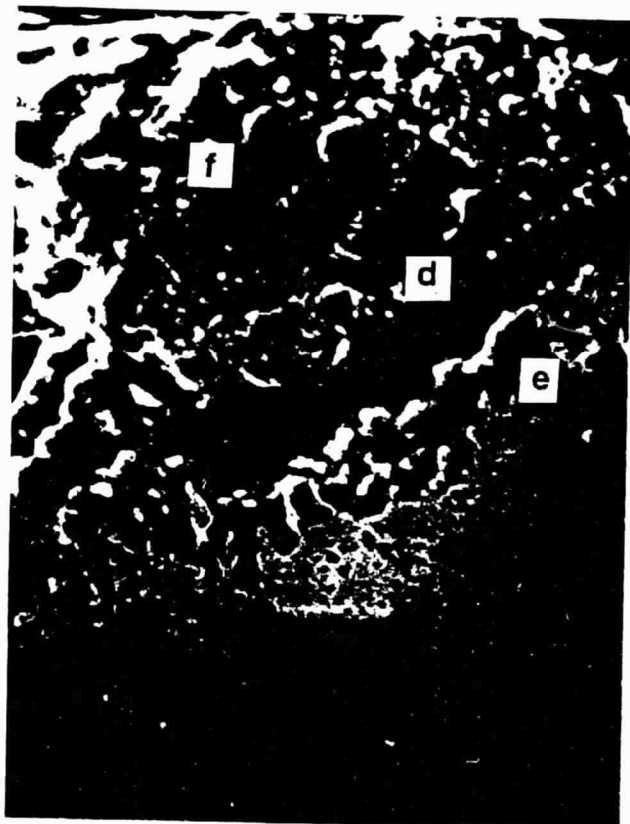
d
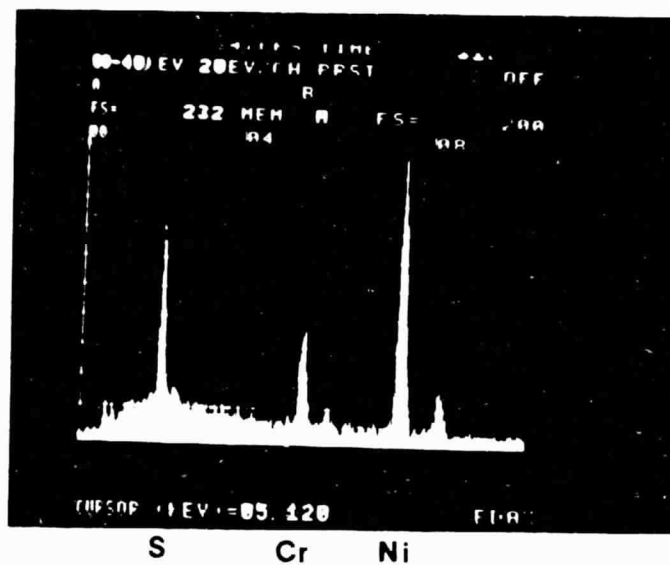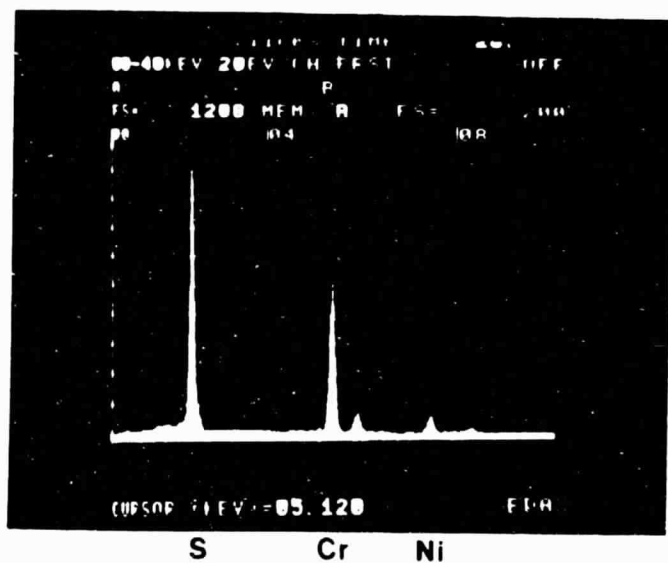
e   f
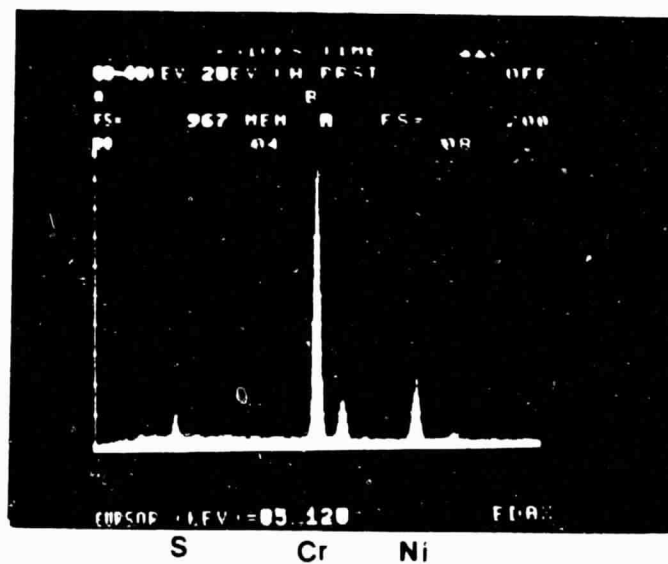
Figure 3. (Cont'd.)
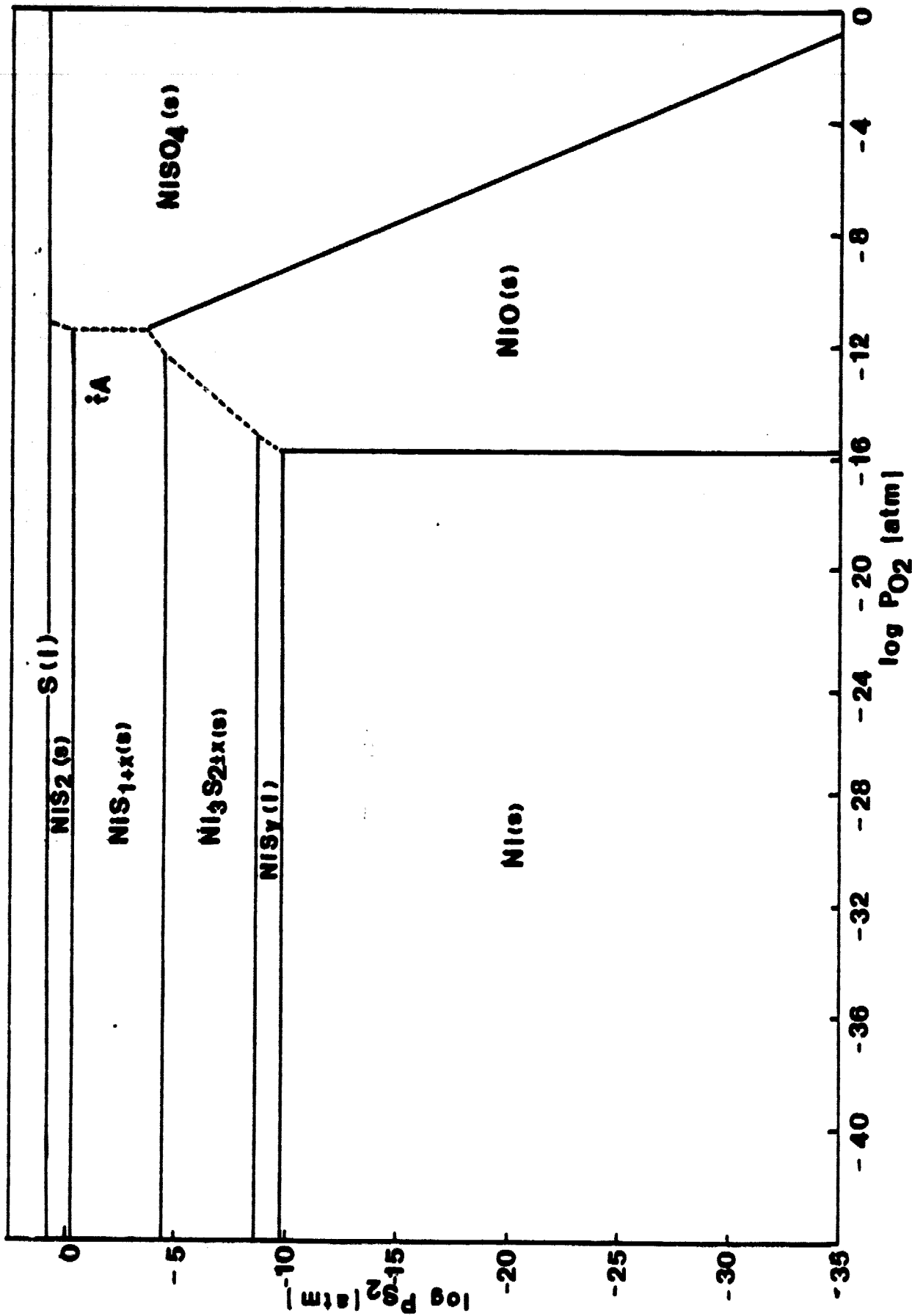
Figure 5.   Stability diagram for the Ni-S-O system at 1000°K.
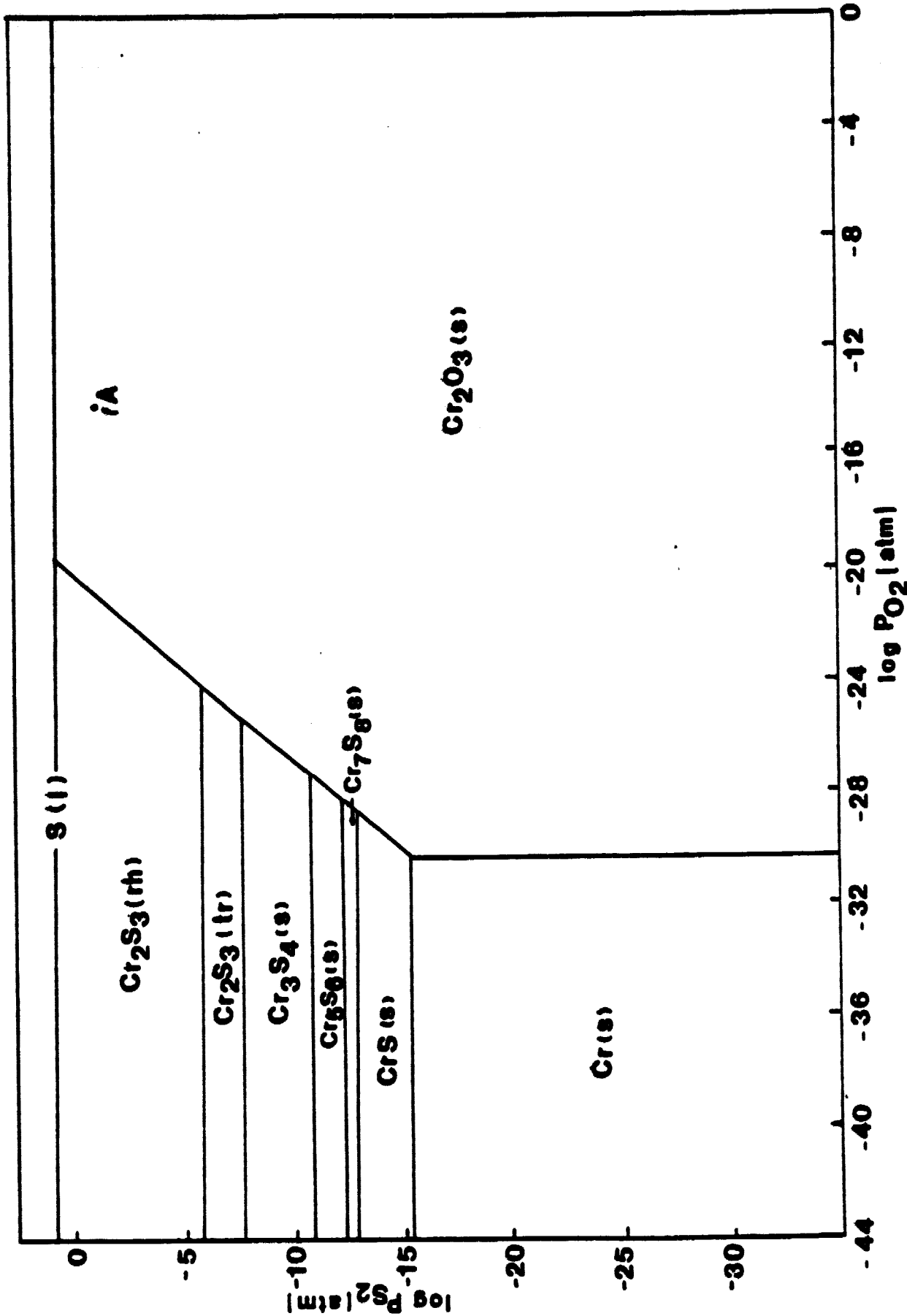
Figure 6. Stability diagram for the Cr–S–O system at 1000°K.
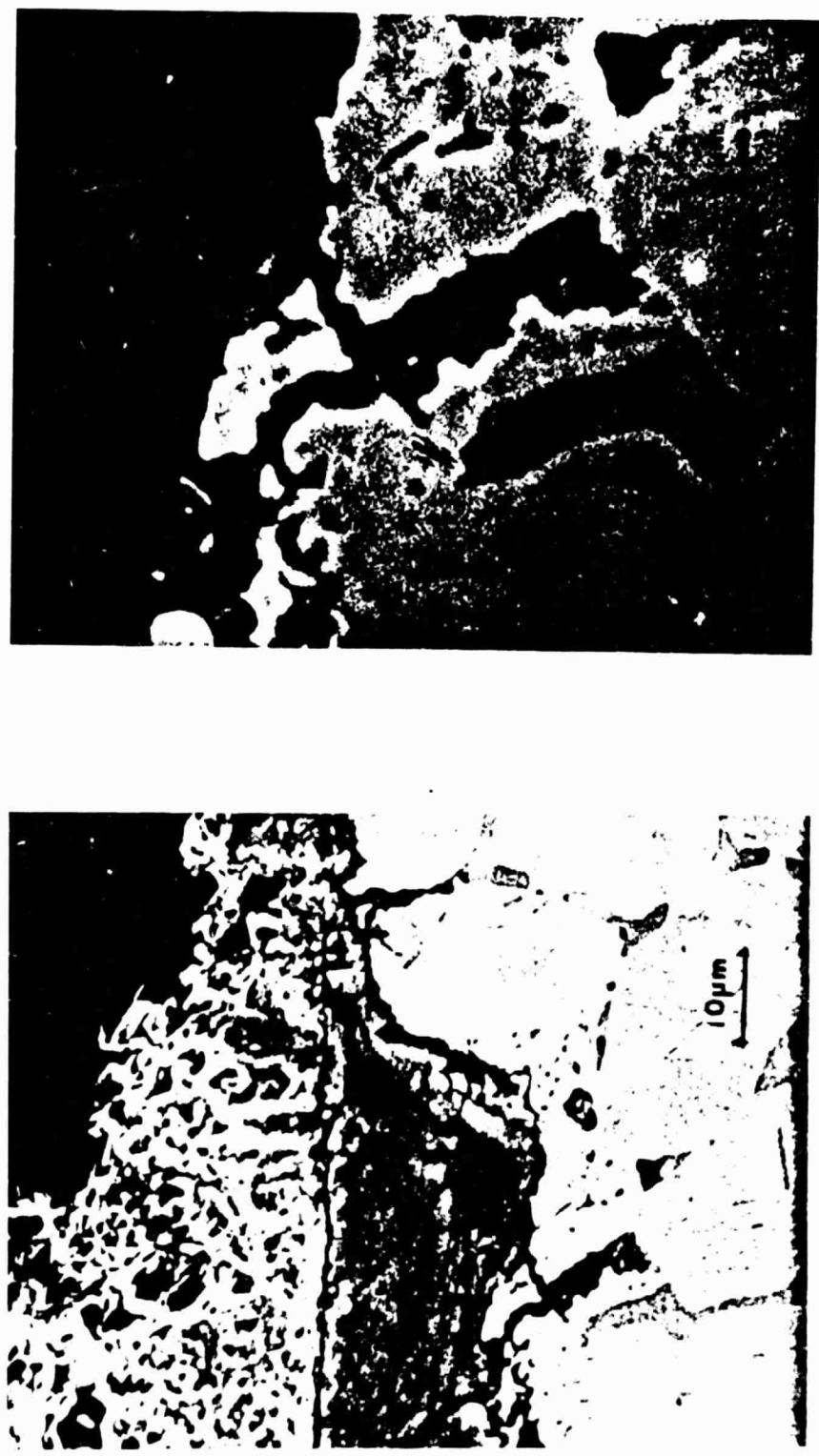
Figure 7. Corrosion morphology for Na_2SO_4-coated Co-18Cr-6Al exposed to $O_2 + SO_3$ ($p_{SO_3} = 2 \times 10^{-3}$ atm) for 48 hours at 750°C.

a, b. Scanning electron micrographs.
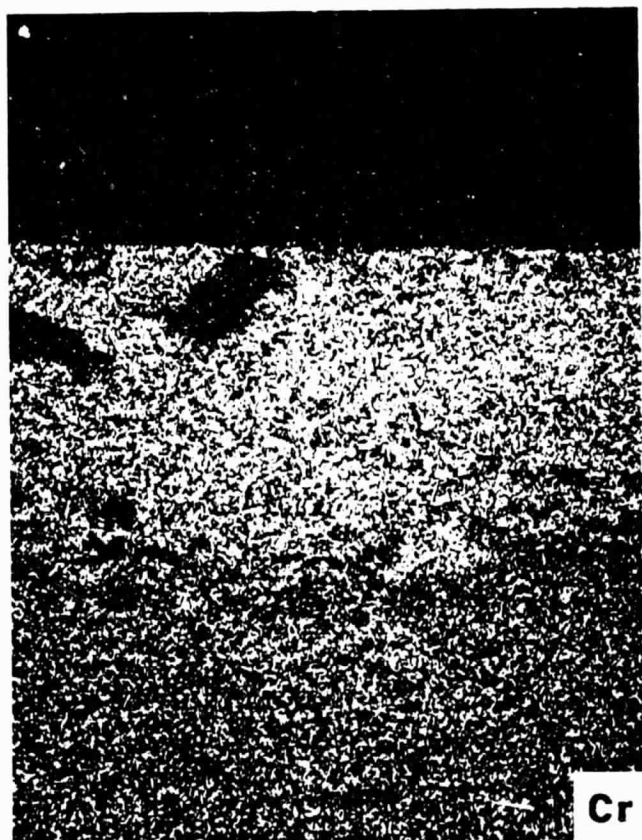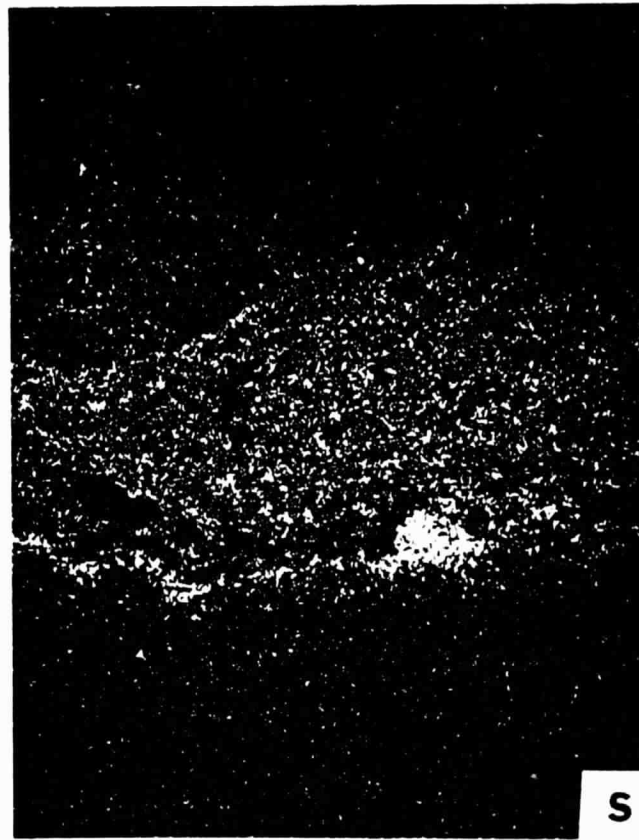
c, d, e, and f. Co-, Cr-, Al-, and S X-ray maps of a.

c

d

Co

Cr

Al

S

e

f
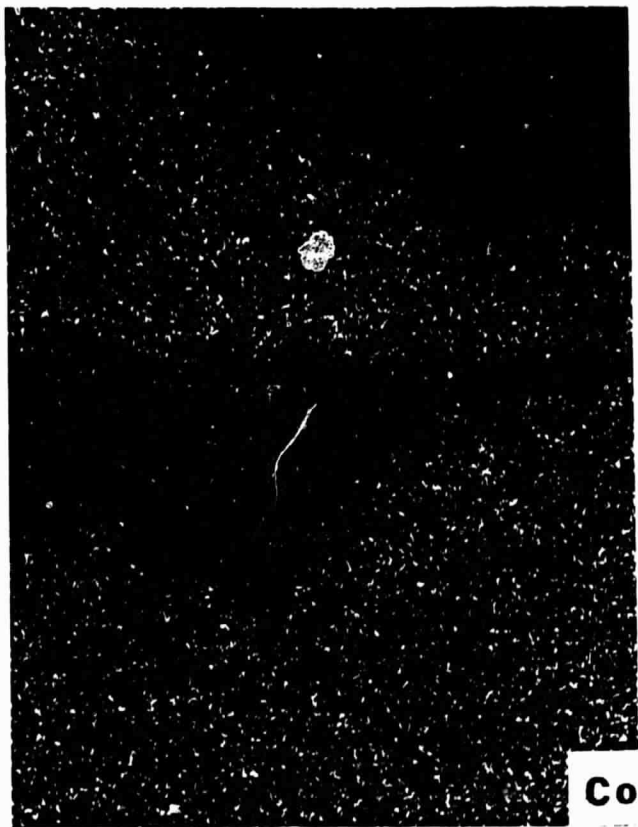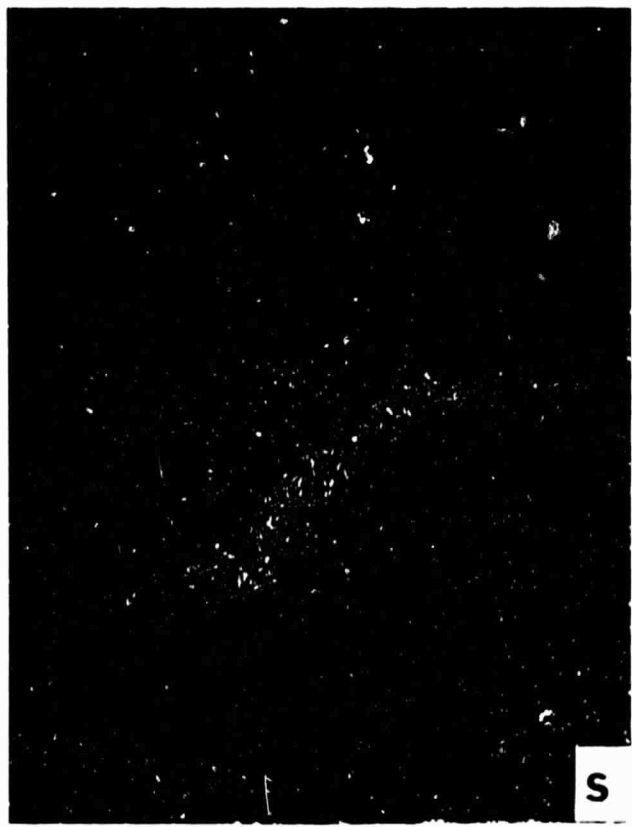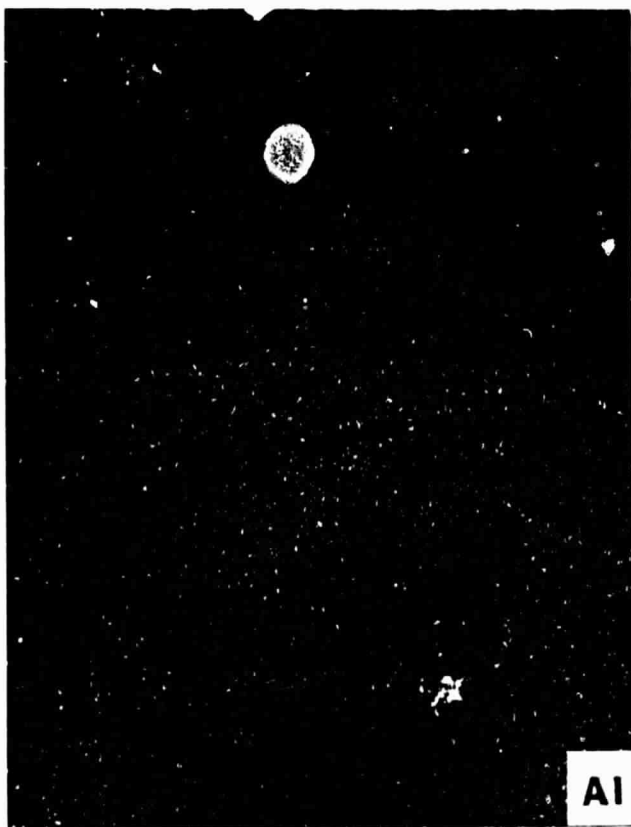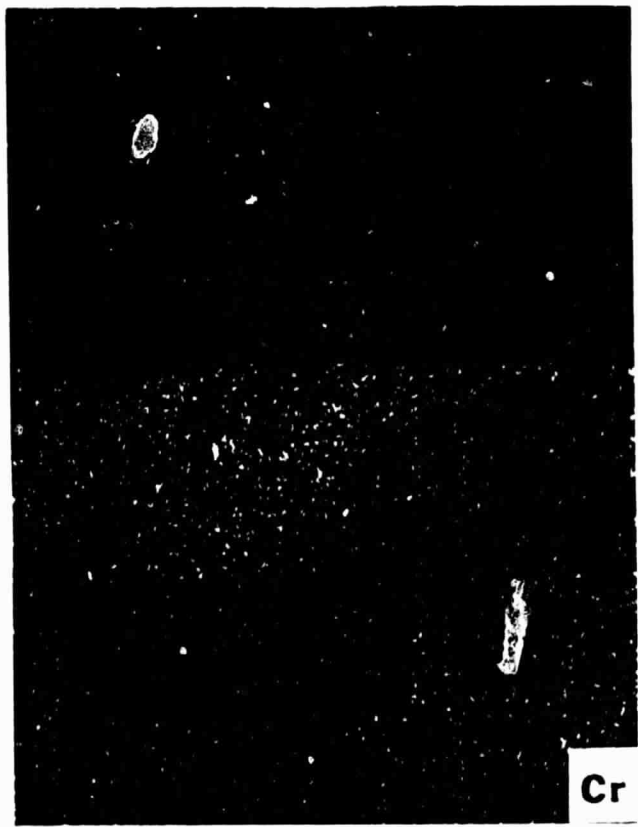
Figure 7. (Cont'd.)
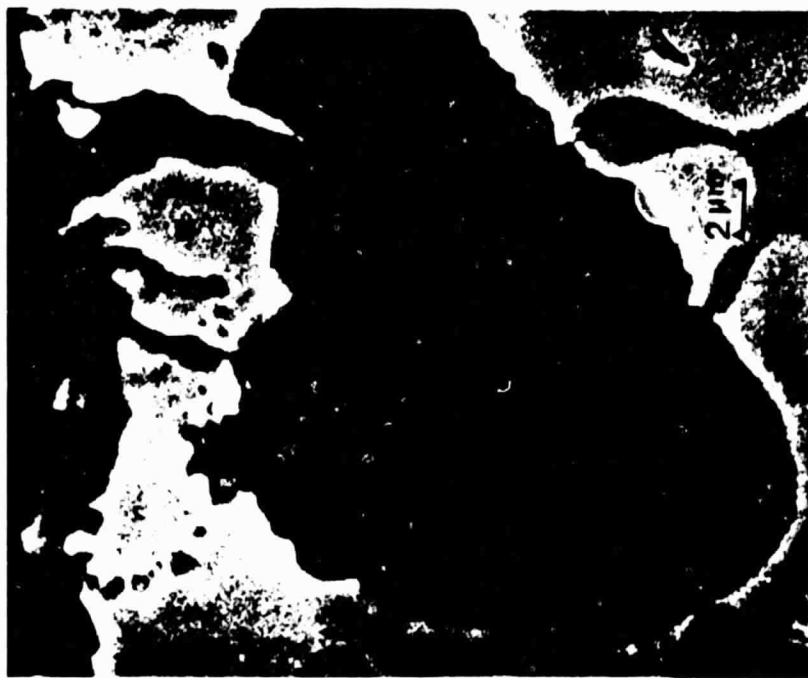
Figure 8. Corrosion morphology for Na_2SO_4-coated Co-18Cr-6Al exposed to O_2 + SO_3 (P_{SO_3} = 2 x 10^{-3} atm) for 4 hrs. at 750°C.

a, b. Scanning electron micrographs.

c, d, e, and f. Co, Cr, S, and Al X-ray maps of b.

Figure 4. Scanning electron micrograph of specimen in Fig. 3(a) and
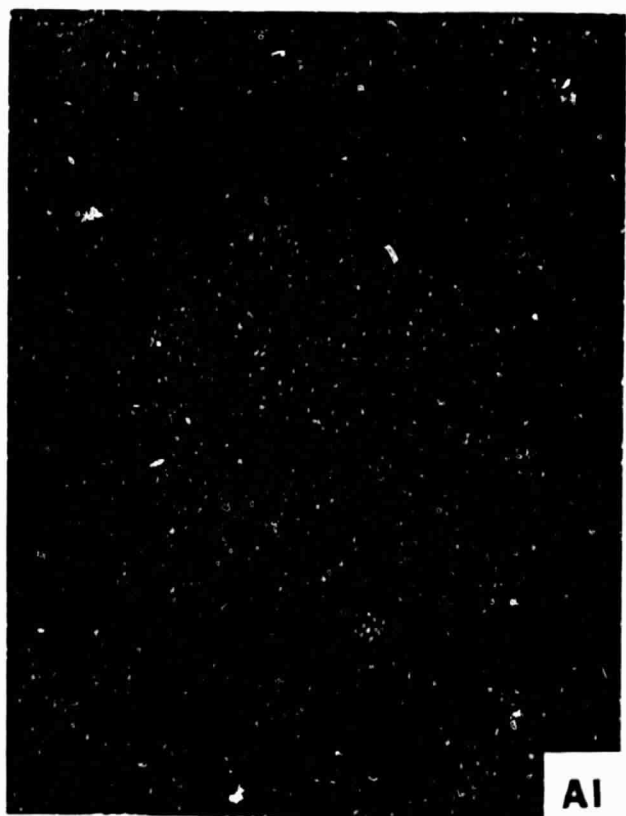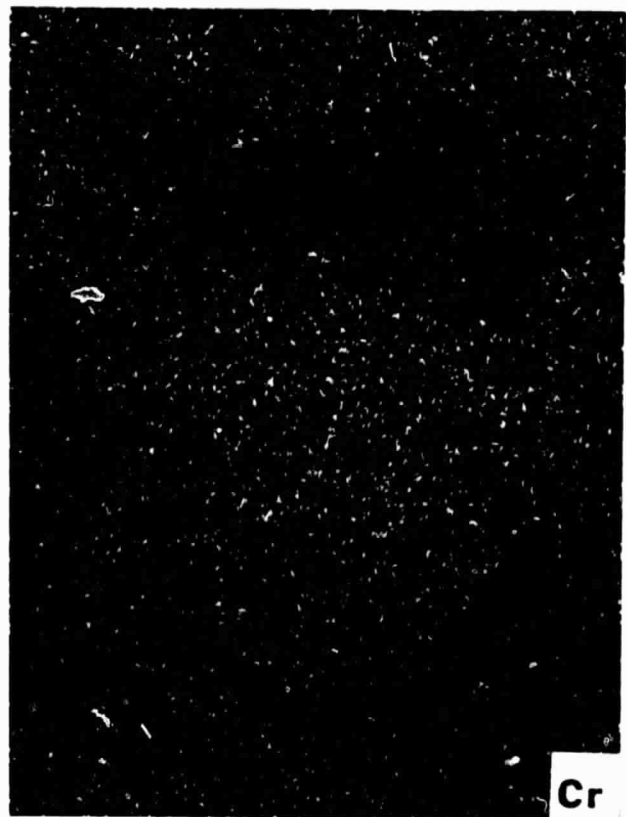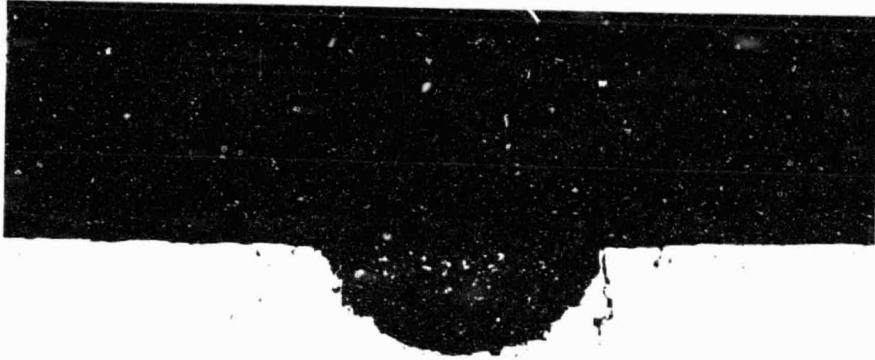Ni (b), Cr (c), and S (d), X-ray maps.
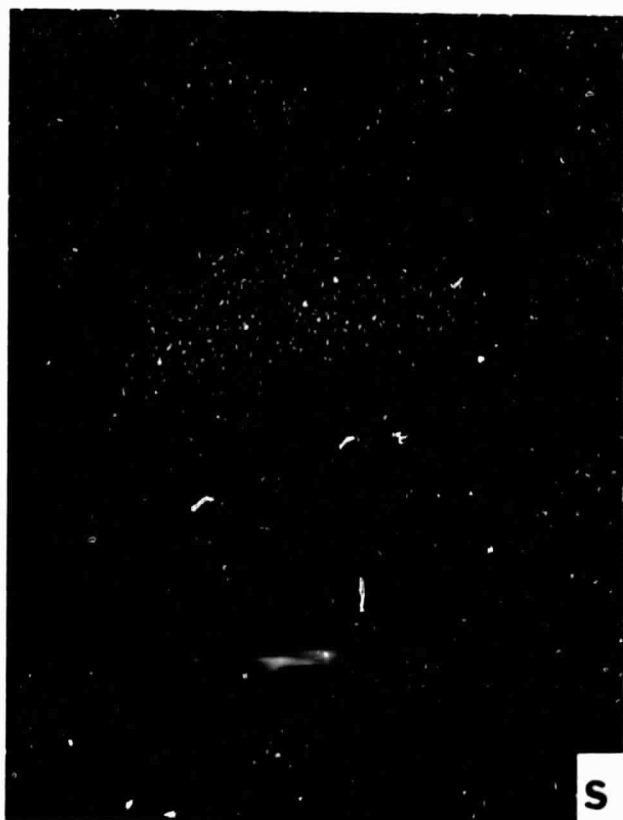
Figure 8. (Cont'd.)

Figure 9. Pitting of Co-18Cr-6Al-1Hf produced in the absence of Na$_2$SO$_4$ by a high p_{S_2}, low p_{O_2} gas.